JMEPEG (2010) 19:46–51
DOI: 10.1007/s11665-009-9412-z

1059-9495/$19.00

Formation of Al_2O_3/Al Composites by Directed Melt Oxidation of Al-Si-Zn Alloy

Jingzhong Zhao, Huiping Chai, and Fajian Zhang

(Submitted December 2, 2008; in revised form February 4, 2009)

Observations are presented on the initiation and growth of Al_2O_3/Al composites by the directed melt oxidation of Al-Si alloys containing metallic Zn or using external dopant ZnO. Thermal gravimetric analysis, optical microscopy, and x-ray diffraction analysis were employed to characterize the progress of oxidation and the nature of oxidation products. Both Zn and ZnO dopants were able to initiate the directed melt oxidation of Al-Si alloys without any Mg being present. Al_2O_3/Al composites were produced when the alloying Zn concentration exceeding 3 wt.%. The incubation period of the oxidation process for Al-Si-Zn alloys was shortened markedly and the amount of composite products increased with the increasing of Zn content in the alloy. In addition, doping with ZnO powder resulted in dense composite formation. A macroscopically planar surface and a fine microstructure promote oxidation growth in Al_2O_3/Al composites. Doping with ZnO powder offers a significant advantage over using metallic Zn for the directed melt oxidation of Al-Si alloy.

Keywords Al_2O_3/Al composites, directed oxidation, dopants, TG analysis

1. Introduction

Al_2O_3/Al composites can be produced by the directed melt oxidation of certain Al alloys (Ref 1, 2). Molten Al alloys can be oxidized by oxygen in air and the Al_2O_3 matrix grows away from the original Al surface toward the air. Liquid Al alloys are continuously supplied to the reaction fronts (air/ceramics interfaces) through interconnecting channels in the Al_2O_3 matrix. Two methods may be used for addition of dopant species needed to promote directed oxidation, the dopants are either applied on the top surface of the parent metals exposed to the oxidants, or, if it is soluble, they are alloyed with parent metals.

Previous investigation (Ref 3-7) on directed melt oxidation involved the oxidation of molten Al-Mg-Si alloys to form Al_2O_3/Al composites. Initially, it was considered that the presence of both Mg and Si in the alloys was necessary for the reaction to occur. The alloying elements play a critical role in preventing the formation of a protective alumina layer on the surface of the melt and in promoting the further oxidation of Al. $MgAl_2O_4$/MgO surface oxides control the oxygen supply to the underlying Al melt. The presence of these non-protective oxides on the surface leads to the sub-surface growth of alumina.

Jingzhong Zhao and **Huiping Chai**, School of Material Science and Engineering, Xi'an University of Technology, Xi'an 710048, P.R. China; and **Fajian Zhang**, Virginia Polytechnic Institute & State University, Blacksburg, VA 24061-0356. Contact e-mails: zjz_63@163.com and sallychai814@yahoo.com.cn.

On the other hand, external dopants placed on top surface of the molten Al alloys simplify the preparation of directed melt oxidation reaction greatly. SiO_2 had been used as a surface dopant with Al-Mg alloys (Ref 8). Using of lithium and magnesia as external dopants promotes the directed oxidation growth successfully (Ref 9, 10). Sindel and Nahum (Ref 11) used spinel ($MgAl_2O_4$) as a surface dopant to initiate the directed oxidation of an Al-Si.

Nagelberg (Ref 12) reported on the growth of Al_2O_3/Al composites from an Al-2.8Zn-0.25 Mg-8.8Si-3.1Cu-1.1Fe alloy at temperatures of 1273 to 1473 K in atmospheres of 20-100 vol% O_2 (balance Ar or N_2) using SiO_2 as an initiator. In this case, the growth mechanism involves the presence of a thin layer of ZnO at the outer surface. The estimated activation energy for composites growth in this alloy, ~89 kJ/mol, is significantly lower than values reported for Al-2.85 Mg-5.4Si and Al-3 Mg-10Si, which range from ~270 to ~400 kJ/mol. This indicates that the complex alloy may be oxidized at relatively higher rates using lower temperatures than those necessary for the Al-Mg-Si alloys. Indeed, Vlach et al. (Ref 13) measured an oxidation rate of ~7 μg/cm^2/s for Al-2.85 Mg-5.4Si at 1373 K, whereas Nagelberg (Ref 12) reported ~50 μg/cm^2/s at the same temperature for the complex zinc-bearing alloy. Hanade et al. (Ref 14) further revealed that composites growth can be promoted by the addition of Zn with relatively high vapor pressure, which forms a metastable surface of oxide ZnO that prevents the passivation of the melt and controls the supply of oxygen to the reaction interfaces. ZnO and $ZnAl_2O_4$ have been placed on top surfaces of molten metals to promote directed oxidation growth (Ref 15, 16).

The present study aims at investigating the mechanisms of initiation and growth of Al_2O_3/Al composites by the directed melt oxidation process, and evaluating the roles of Zn or ZnO dopants in the oxidation process and the microstructure.

2. Experimental Procedure

To study the effect of metallic Zn on the oxidation behavior of Al-Si alloys, various Al-Si-Zn alloys (Table 1) of similar composition with varying Zn content were prepared using a commercial ZLD104 alloy (QingHai Aluminum Factory, China; its chemical components are shown in Table 2) and commercial purity Zn (99.92%). All alloys were melted in an electric resistance furnace at the temperature of 750 °C for 30 min, and then the melts were casted into some rods of 15 mm diameter. These rods were subsequently sectioned into 10-mm length using a low-speed diamond saw, and their surfaces were ground with SiC paper down to a 600 grit followed by polishing to remove the native alumina.

Figure 1 shows the apparatus that can continually measure the weight gain during the directed oxidation. A vertical tube furnace was used as the reaction chamber. The cylindrical specimens were embedded into barrier powder in an alumina crucible and only the top surface of the specimen was directly exposed to the atmosphere. The crucible and its content were suspended by a Pt wire and placed into a furnace where they were heated in air to their setpoint temperature 1100 °C, and kept at this temperature long enough until the experiment was accomplished. During this period, TG28A analysis balance was employed to weigh the beginning weight of the crucible sets and determine the weight increment of specimens. The data were recorded every 5 min until weight increment was <1 mg/min, then we could obtain final weight gain data accumulated increment of different samples. All of the experiments were carried out in ambient atmosphere. The weight gain plots depend on time at constant temperature were charted accordingly.

In order to investigate the effect of ZnO on the directed melt oxidation of Al-Si alloys, ZnO powder was placed on top surface of the ZLD104 alloy as an external dopant. Weights of ZnO powder as different samples are shown in Table 3. Again, thermal gravimetric analysis was performed as described above.

The resulting samples were cut out using a low-speed diamond saw, their cross sections were ground and polished with diamond paste. The phases of composite samples were quantitatively analyzed using X-ray diffraction (XRD, science D/MAX-RA diffractemeter, Cu $K\alpha$ radiation) and the microstructure observation was carried out using optical microscopy and scanning electron microscopy (SEM; Model No. S-5000, Hitachi Co., Ltd., Tokyo, Japan).

Table 1 Al-Si-Zn alloy containing different Zn contents

Sample	Alloy	Actual Zn content, wt.%
a	Al-9Si	0.25
b	Al-9Si-Zn	1.03
c	Al-9Si-3Zn	2.72
d	Al-9Si-5Zn	4.91
e	Al-9Si-7Zn	6.86
f	Al-9Si-10Zn	9.67

Table 2 Chemical components of the ZLD104 alloys

Element	Mg	Si	Zn	Cu	Ti	Fe	Mn	Cr
Wt.%	0.31	9.2	0.25	0.1	0.15	0.37	0.31	0.05

Table 3 Weight of ZnO surface dopant

Sample	A	B	C	D
ZnO (mg/cm^2)	22	31	40	54

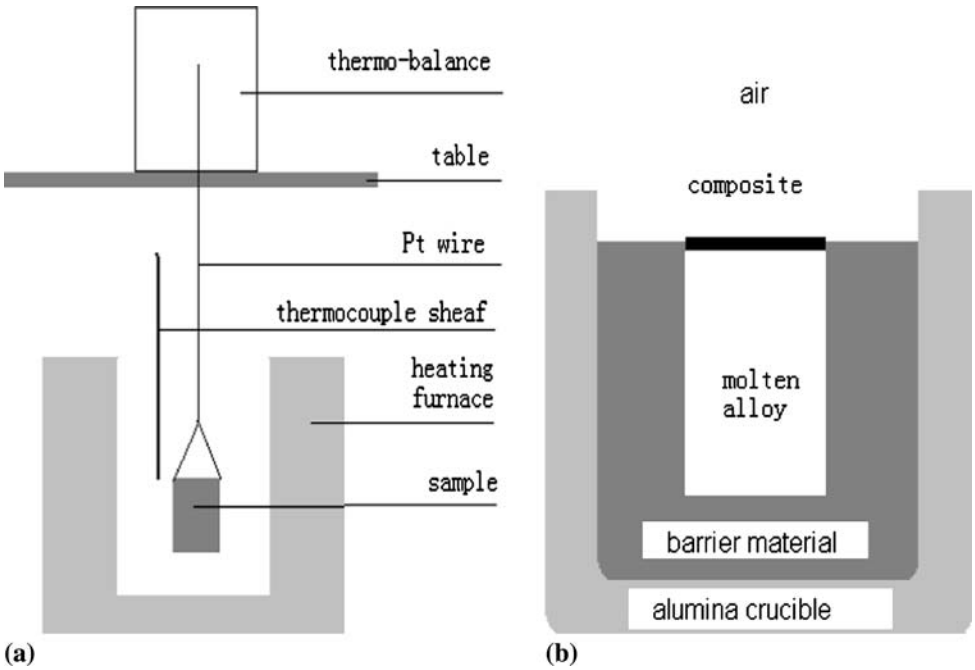

Fig. 1 The experimental arrangement for the thermo-gravimetric experiments. (a) The experimental arrangement and (b) the crucible scheme

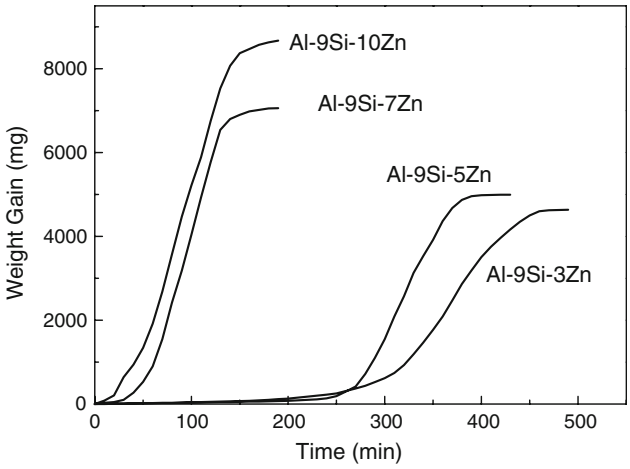

Fig. 2 Weight gain vs. reaction time results for Al-Si-Zn alloys containing different amounts of metallic Zn at 1100 °C

3. Results

3.1 Samples Initiated with Alloying Zn

Figure 2 shows the TGA plots for six alloy samples listed in Table 1. When Zn content was 1 wt.% or lower, oxidation could not be started, apparent oxidation was observed when Zn content were 3, 5, 7, and 10 wt.% at 1100 °C, and accordingly the oxidation weight gains were 4633, 4996, 7060, and 8670 mg. It can also be seen from Fig. 2 that in the second stage overall, the growth rate of specimens increased with the increment of Zn content in the alloy. The reason is that the vapor pressure of element Zn become higher with the increasing Zn content in the molten alloy at high temperature, then there are more Zn diffusing to the alloy surface and reacting with oxygen in the air. Consequently, more yellow powder zinc oxide was formed which kept the reactions (2), (3), and (4) cycled, and thus more composite matrices are formed.

By observing the cross sections of grown products, yellow surface layers were found on top of the products, the thickness of the layer was about 1 mm. Beneath the yellow layer, there was a discontinuous powdered layer and the thickness of which was variable in different regions. The thickest part of the layer was at the top of the hemispherical mound, while the thinnest part was near the transitional regions. There was no powdered layer at the contact boundaries. The hard matrix was beneath the powder layer. XRD analysis of the yellow surface layer indicated that this layer consisted mainly of ZnO and a small quantity of $ZnAl_2O_4$ (Fig. 3), the powdered layer was almost all ZnO (Fig. 4). However, XRD (Fig. 5) shows that the composite matrix contains α-Al_2O_3, Al, Si, and $ZnAl_2O_4$; no Zn or ZnO was detected.

3.2 Samples Doped with ZnO

Figure 6 shows the TGA measurement results of the samples doped with different amounts of ZnO powder. For the sample doped with 22 mg/cm^2 of ZnO, very slight oxidation weight gain was detected after heating to 1100 °C for 420 min. While 31, 40, or 54 mg/cm^2 of ZnO were used to dope the ZLD104, complete oxidation of alloy surfaces was observed. Thin yellow layers covered the surfaces of these samples and there were no dopant remained. The sample doped with 31 mg/cm^2 of ZnO

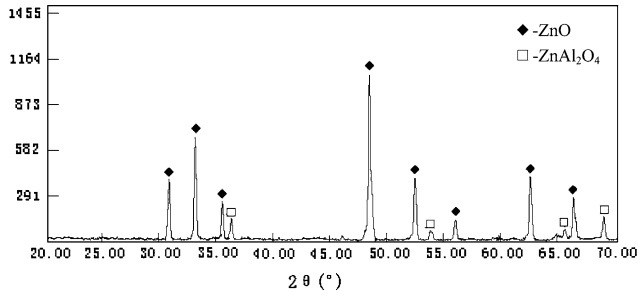

Fig. 3 XRD pattern of yellow compound on the surface of sample d

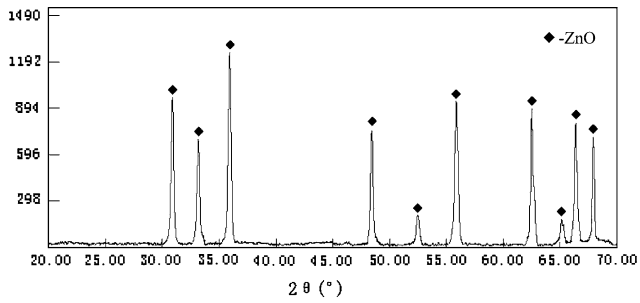

Fig. 4 Powder XRD pattern of powder layer beneath yellow crust of sample d

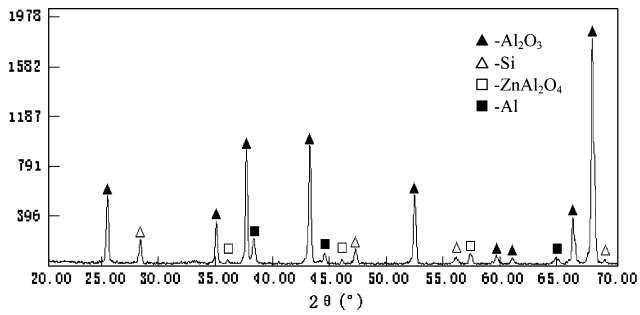

Fig. 5 XRD pattern of composite layer of sample d

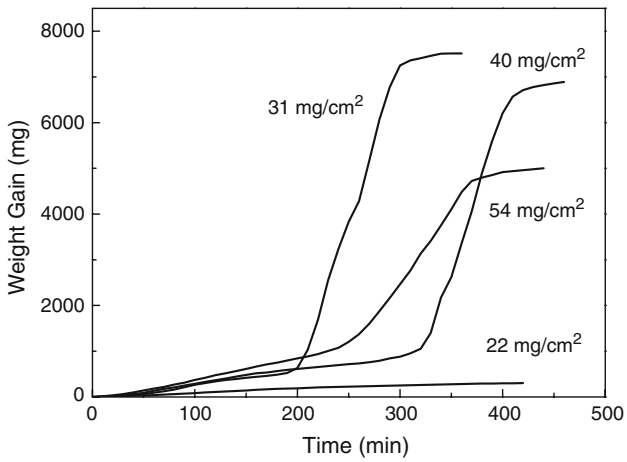

Fig. 6 Weight gain vs. reaction time at 1100 °C of ZLD104 alloys doped with different amounts of ZnO

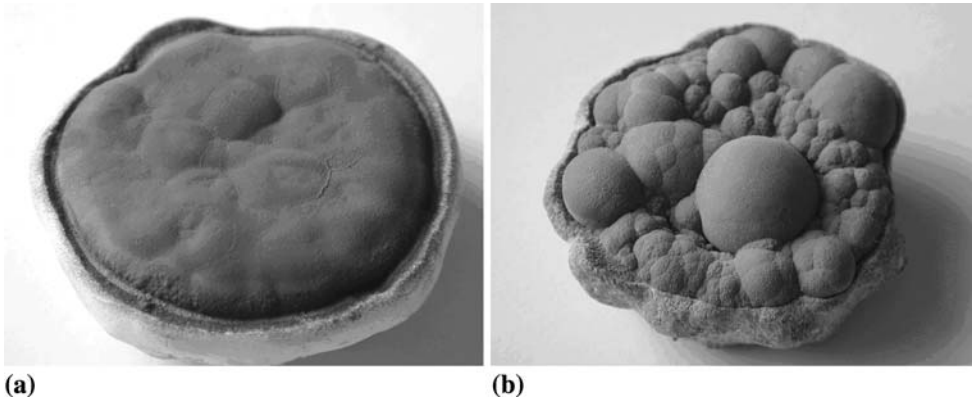

Fig. 7 Morphologies of growth surfaces. (a) Sample d and (b) sample c

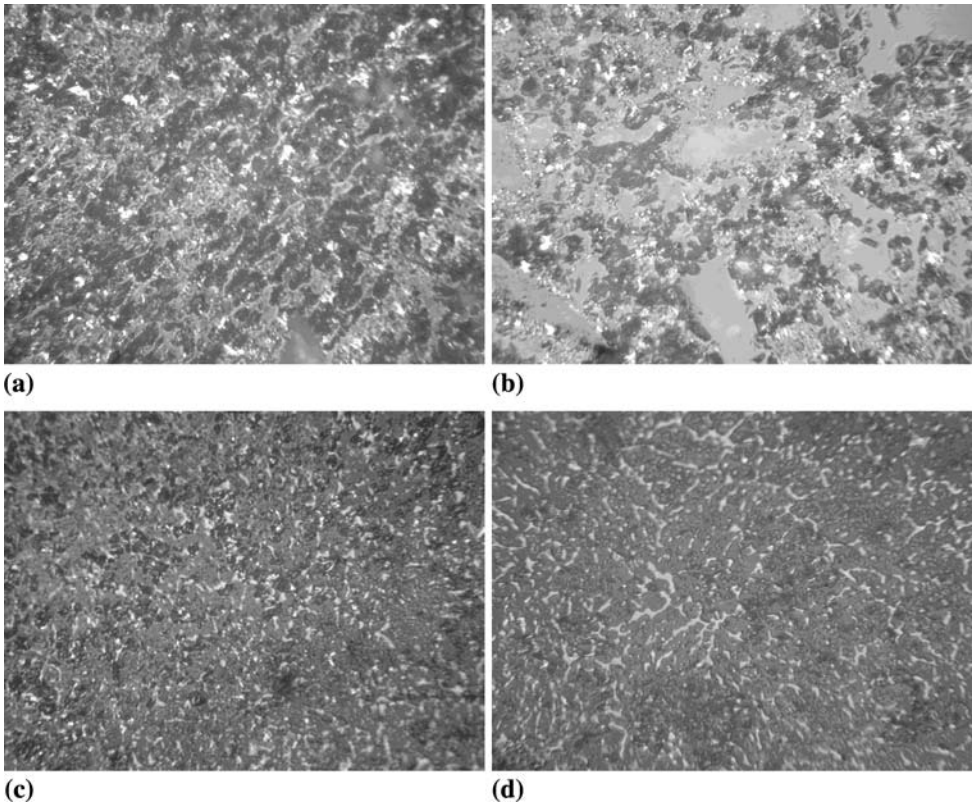

Fig. 8 Surface features of composites observed by optical microscopy. (a) Sample d, (b) sample c, (c) sample d, perpendicular to the growth direction. (d) Sample d, parallel to the growth direction

was the best, its oxidation weight gain reached 1516 mg and incubation period took only 200 min, which is even better than that of Al-9Si-5Zn alloy as shown in Fig. 2.

3.3 Morphologies and Microstructures

Figure 7(a) shows the rough surface morphology of the composites produced by the directed oxidation of Al-9Si-5Zn alloy at 1100 °C (sample d), the macroscopic surface consists of hemispherical mounds 0.1-3.0 mm in diameter, and the size of the mounds are evidently different. The morphology of ZLD104 alloy doped with 31 mg/cm^2 ZnO powder (sample c) is shown in Fig. 7(b). There is an obvious morphology change of the top surface in sample c compared with that of sample d, while the surface morphology becomes uniform and develops undulations in the form of ripples. This indicates that metallic Zn was replaced by ZnO powder doped on the alloy surface, all of the mounds become thinner in some extent, and the growth surfaces tend to be smooth.

Figure 8(a, b, and d) are the cross-sectional images of sample d at perpendicular and parallel directions with respect to the growth direction. It is found that instead of metallic Zn, it is ZnO dopant that caused a remarkably big gray ceramic phase (ripples), while the metal phase became obviously thin and uniformly distributed, the number of black cavities decreased, too. Being distributed among the gray ceramic matrix phase, the

white metal phase looks like "islands." Figure 8(d) is the optical image of the sample d oriented parallel to the growth direction. It is found that the white metal phase is two-dimensionally connected, which directly shows the unidirectional grow character of directed oxidation of molten metal. The composite matrix consists of three-dimensional α-Al_2O_3 matrix networks, netted metals (Al, Si), and some remnant voids.

From Fig. 7 and 8, we can know that the outside surface of the composite product is flat, while the inner structure of which is three-dimensionally connected. When the temperature reached the reaction temperature, growth of the composites begun. At first, the alloying element Zn diffused to the surface of molten alloy and reacted with oxygen in the air to form zinc oxide, which can react with the Al liquid to form Al_2O_3 and $ZnAl_2O_4$, reactions as (2), (3), and (4). Gradually, with the forming of more Al_2O_3 ceramic matrix, the thickness of the composites became larger and the surface of the composites formed as shown in Fig. 7(b) was pushed toward the air direction. And the drive force of the growth of the composites is the continuous supply of molten Al liquid through the microchannel which formed the capillary force. Finally, when the composite growth stopped, the microstructure of the composites as shown in Fig. 8 is the gray ceramic Al_2O_3 matrix with the white netted residual Al-Si metal phase distributed in it.

4. Discussion

Figure 2 shows the TGA plots for Al-Si-Zn alloys at 1100 °C, the weight gain rate was found to be dependent on the alloying Zn content (oxidation could not be started if Zn content was 1 wt.% or lower). It was also seen that samples containing different amounts of metallic Zn resulted in different initiation times, whereas similar general oxidation behaviors were observed, since their microstructure evolution followed the same pattern. The growth of Al_2O_3/metal composites by the directed oxidation of Al-Si-Zn alloys proceeded through three distinct stages (Ref 16): the incubation period, the rapid growth period, and the saturated growth period. The following reactions occurred during these stages.

The first stage was the incubation period, which started from the moment the alloy specimen was placed into the furnace. The presence of Zn with higher vapor pressure may help in breaking the native oxide and diffuse to react with oxygen in the air to form yellow ZnO powder.

$$2Zn(g) + O_2(g) \rightarrow 2ZnO(s) \quad \text{(Eq 1)}$$

ZnO powder is fragmented, which could allow Zn vapor to escape and oxidize. Two types of reaction involving the liquid Al and ZnO can be envisaged, one is the formation of intermediate spinel $ZnAl_2O_4$, the other is the reduction of ZnO to element Zn:

$$2ZnO(s) + 4Al(l) + 3O_2(g) \rightarrow 2ZnAl_2O_4(s) \quad \text{(Eq 2)}$$

$$3ZnAl_2O_4(s) + 2Al(l) \rightarrow 4Al_2O_3(s) + 3Zn(g) \quad \text{(Eq 3)}$$

or

$$3ZnO(s) + 2Al(l) \rightarrow Al_2O_3(s) + 3Zn(g) \quad \text{(Eq 4)}$$

Both the spinel and ZnO are extremely metastable compared with alumina, when in contact with the molten Al alloys. Therefore, the interfacial reactions seem to be the mechanism by which alumina was formed. As the case of Al-Mg based alloy (Ref 4, 6), the alumina was formed by dissolution of oxygen at the Al-ZnO interface and re-attachment after reaction at the Al-Al_2O_3 interface. This process obviates the need of re-nucleation of alumina on zinc oxide. However, diffusion couples between molten alloy and sintered ZnO carried out continuously, while the initial reaction product of alumina could not form a continuous layer. Consequently, molten Al could not be transported to the reaction front until the formed alumina/aluminum composites were thick enough to have sufficient capillary force for the transportation of molten Al, then reactions (1), (2), (3), or (1), (4) can go along repeatedly. During the incubation period, the Al_2O_3/Al composites layer thickened slowly, it took a long time to form the composites film which is thick enough for transporting the molten Al. Therefore, the oxidation rate in this stage is relatively lower. This can be seen from the smooth part of the weight gain rate curve.

The second stage was the rapid growth period, the cyclic reactions carried on rapidly, which made the ZnO layer moved toward the direction of air, and the Al_2O_3/Al composites layer beneath the ZnO layer continued to thicken as the time prolonged, some microchannels formed gradually inside this layer. Under the control of the capillary force, molten Al alloy was transported continuously to the reaction front along these microchannels, which made alumina persistently grow toward the surface. Figure 2 shows that the slope of the curves fairly increased during the second stage, and became straight lines overall, constant rate of growth was observed in this stage.

In the third stage, the corresponding growth curve tended to be flat, the growth was very slow, or even stops. This was the saturating growth stage. Because most of the molten Al has been depleted during the second stage, the supply of molten Al was exhausted. Reactions could not proceed.

In contrast to some previous results (Ref 11, 17), metallic Zn was found to be capable of initiating directed melt oxidation in all cases. In this study, however, the ability of Zn content (≤3 wt.%) in Al alloy was found to be different in promoting the oxidation reaction.

It is seen from Fig. 2 that the incubation period is shortened and the growth rate in the second stage tends to increase with increasing metallic Zn. The incubation period of alloys with 10% Zn content is slightly shorter than that of an alloy with 7% Zn, but their oxidation growth rates are basically the same. A higher Zn content in molten alloy at high temperature can cause a higher vapor pressure of Zn, rapid corrosion of the power film, and increasing weight gain. This promoted the above-mentioned cyclic reactions and reduced the period of time needed for forming a film thick enough to cause capillary force. For these reasons, the alloy of 3% Zn content had the longest incubation period, while the alloy of 10% Zn content had the shortest.

When Al in the alloy arrives at Al-ZnO interface and contacts with metastable ZnO, reactions (2), (3), or (4) occur to produce solid alumina, which release gaseous Zn. The Zn vapor diffuses away from the newly created alumina toward the top of the system, and Zn can re-oxide to form ZnO. All reactions occur near the entrances of the microchannels. This will result in different microchannel diameters, different transporting rates, and resistance of molten alloy in each channel. Small amount of microchannels is dominant, which transported most of the molten alloy to the reaction fronts. Near the entrances of these microchannels, the thickness of Al_2O_3/Al composite matrix and

powdered ZnO crust layer took on hemispherical distribution (Fig. 7). The cellular hemisphere had more chances to react in touch with oxygen, so cell-like surface mounds became bigger and bigger. This is so-called preferential growth.

When ZnO powder is placed on the top surface of the ZLD104 alloy as an initiating dopant at high temperature, reaction (4) will occur first at the molten Al-ZnO interfaces. Similar cyclic reactions are expected to happen and go on. The thickness of the surface dopant layers will control the Zn vaporization to the top of the system and oxygen supply to the underlying Al melt. When the quantity of ZnO powder is <22 mg/cm^2, a small amount of the composites is produced, which is insufficient to form the desired thickness by which the liquid metal supply is maintained to the reaction fronts, so the oxidation growth process stops during the incubation stage. The small amount and thin layer of ZnO dopant will promote the cyclic reactions, which means shorter incubation time. With the increasing of ZnO dopant (22-40 mg/cm^2), the surface layer thickens. Reaction (3) goes on continuously, and the vapor pressure of Zn becomes higher and higher. The composite growth relies on the diffusion of ions through the external ZnO layer. The incubation period will lengthen, but their oxidation rates are similar. When the quantity of ZnO powder is up to 54 mg/cm^2, oxygen supply would not satisfy the rapid reaction growth, because the surface layer is too thick. Oxidation growth rate would slow down, which implies a longer incubation period. This event corresponds to a decline slope in the curve of weight gain rate as shown in Fig. 6.

When external ZnO instead of metallic Zn is used as a dopant, less porous composite products will be obtained. When Zn is supplied by ZnO, it is less readily vaporized and thus the vapor pressure of Zn is lower at any stages. This means that Zn is less readily transported away from the main reaction fronts, and oxide/metal composites continuously grow with a macroscopically planar surface. This coincided with a morphological change at the surface and the formation of an Al_2O_3/Al composite layered structure at the surface. Correspondingly, using metallic Zn as a dopant will lead to the continuing generation of high Zn partial pressure. The composite produced will have higher porosity.

5. Conclusions

(1) Al_2O_3/Al composites can be produced when alloying Zn concentration increased to 3-10 wt.% at 1100 °C. The incubation period of the oxidation process for Al-Si-Zn alloy is reduced and the amount of the products increases with the increasing of Zn content.

(2) Al_2O_3/Al composites can be successfully produced by doping with 31-54 mg/cm^2 ZnO powder on the surface of ZLD104 alloy. The optimum value of the ZnO dopant is 31 mg/cm^2.

(3) Doping with ZnO powder offers a significant advantage for the directed melt oxidation of Al-Si alloys over using metallic Zn. Doping with ZnO powder results in dense composite formation, and it produces the Al_2O_3/Al composite oxidation growth with a macroscopically planar surface and a fine microstructure.

Acknowledgments

We are grateful for the financial support from Natural Science Foundation of Shaanxi Province of P.R. China (Grant No. SJ08-ZT05) and Education Department of Shaanxi Province of P.R. China (Grant No. 07JK359).

References

1. M.S. Newkirk, A.W. Urquhart, and H.R. Zwicker, et al., Formation of Lanxide™ Ceramic Composite Materials, *J. Mater. Res.*, 1986, **1**, p 81–89
2. A.W. Urquhart, Novel Reinforced Ceramics and Metals: A Review of Lanxide's Composite Technologies, *Mater. Sci. Eng.*, 1991, **A144**, p 75–82
3. A.S. Nagelberg, Observation on the Role of Mg and Si in the Directed Oxidation of Al-Mg-Si Alloy, *J. Mater. Res.*, 1992, **7**, p 265–268
4. S. Antolin and A.S. Nagelberg, Formation of Al_2O_3/Metal Composites by the Directed Oxidation of Molten Aluminum-Magnesium-Silicon Alloys: Part 1, Microstructural Development, *J. Am. Ceram. Soc.*, 1992, **75**, p 447–454
5. A.S. Nagelberg and S. Antolin, Formation of Al_2O_3/Metal Composites by the Directed Oxidation of Molten Aluminum-Magnesium-Silicon Alloys: Part II, Growth Kinetics, *J. Am. Ceram. Soc.*, 1992, **75**, p 455–462
6. E.C. Partington and P. Grieveson, Self-Sustaining Oxidation of Liquid Aluminum and Its Alloys Containing Magnesium and Silicon, *J. Mater. Sci.*, 1998, **33**, p 2447–2455
7. T. Debroy, A. Bandopadhyay, and R. Roy, Oxide Matrix Composites by Directed Oxidation of a Commercial Aluminum-Magnesium Alloys, *J. Am. Ceram. Soc.*, 1994, **77**, p 1926–1930
8. X.Y. Zhou, J.F. Chen, and J.F. Chen, Effect of SiO_2 on Directed Oxidation of Molten Aluminum Alloy, *Acta Materiae Compositae Sinica.*, 1997, **14**, p 9–14
9. X. Gu and R.J. Hand, The Use of Lithium as a Dopant in the Directed Melt Oxidation of Aluminium, *J. Europ. Ceram. Soc.*, 1996, **16**, p 929–935
10. X. Ping and B. Derby, Alumina/Aluminum Composites Formed by the Directed Oxidation of Aluminum Using Magnesia as Surface Dopant, *J. Am. Ceram. Soc.*, 1994, **77**, p 1761–1770
11. M. Sindel and A.T. Nahum, Influence of Magnesium-Aluminum Spinal on the Directed Oxidation of Molten Aluminum Alloys, *Am. Ceram. Soc.*, 1990, **73**, p 2615–2618
12. A.S. Nagelberg, Growth Kinetics of Al_2O_3/Metal Composites from Complex Alloys, *Solid State Ionics*, 1989, **32-33**, p 783–788
13. K.C. Vlach, O. Salas, and V. Jayaram, et al., A Thermogravimetric Study of the Oxidative Growth of Al_2O_3/Al Alloy Composites, *J. Mater. Res.*, 1991, **6**, p 1982–1995
14. M. Hanade, V. Jayaram, and T.A. Bhaskaran, Growth of Al_2O_3/Al Composites from Al-Zn Alloys, *Acta. Mater.*, 1996, **44**, p 819–829
15. S.Q. Cheng, J.Z. Zhao, and C.Q. Gu, Effect of ZnO Dopant on Direct of Melt Oxidation Growth on the Surface of Aluminum Alloy, *J. Chin. Ceram. Soc.*, 2004, **32**, p 671–674
16. J.Z. Zhao, J.J. Chang, J. S. Yue, and F.J. Zhang, Structure Evolution of Composites Produced by Directed Oxidation of Al-Si-Zn Alloy, *J. Chin. Ceram. Soc*, 2007, **35**(8), p 1007–1012
17. R. Shamsudin and R.J. Hand, Al_2O_3/Al Composites Produced by Directed Melt Oxidation Using Zn Containing External Dopants, *J. Mater. Sci*, 2001, **36**, p 1613–1619